

Direct Gravitational Imaging of Intermediate Mass Black Holes in Extragalactic Halos

Kaiki Taro Inoue^{1*} Valery Rashkov^{2†} Joseph Silk^{3,4,5‡} and Piero Madau^{2§}

¹*Department of Science and Engineering, Kinki University, Higashi-Osaka, 577-8502, Japan*

²*Department of Astronomy and Astrophysics, University of California, Santa Cruz, 1156 High Street, Santa Cruz, CA 95064*

³*Institut d’Astrophysique de Paris, UMR 7095, CNRS, UPMC Univ. Paris VI, 98 bis boulevard Arago, 75014 Paris, France*

⁴*Department of Physics and Astronomy, The Johns Hopkins University Homewood Campus, Baltimore, MD 21218, USA*

⁵*Beecroft Institute for Particle Astrophysics and Cosmology, University of Oxford, Denys Wilkinson Building, Keble Road, Oxford, OX1 3RH, UK*

8 June 2018

ABSTRACT

A galaxy halo may contain a large number of intermediate mass black holes (IMBHs) with masses in the range of $10^{2-6} M_{\odot}$. We propose to directly detect these IMBHs by observing multiply imaged QSO-galaxy or galaxy-galaxy strong lens systems in the submillimeter bands with high angular resolution. The silhouette of an IMBH in the lensing galaxy halo would appear as either a monopole-like or a dipole-like variation at the scale of the Einstein radius against the Einstein ring of the dust-emitting region surrounding the QSO. We use a particle tagging technique to dynamically populate a Milky Way-sized dark matter halo with black holes, and show that the surface mass density and number density of IMBHs have power-law dependences on the distance from the center of the host halo if smoothed on a scale of ~ 1 kpc. Most of the black holes orbiting close to the center are freely roaming as they have lost their dark matter hosts during infall due to tidal stripping. Next generation submillimeter telescopes with high angular resolution ($\lesssim 0.3$ mas) will be capable of directly mapping such off-nuclear freely roaming IMBHs with a mass of $\sim 10^6 M_{\odot}$ in a lensing galaxy that harbours a $O(10^9) M_{\odot}$ supermassive black hole in its nucleus.

Key words: cosmology: theory - gravitational lensing - black hole physics - galaxies: formation

1 INTRODUCTION

Recent observations of off-nuclear ultraluminous X-ray sources (ULXs) suggest the presence of intermediate mass black holes (IMBHs) not only in the neighborhood of the galaxy nucleus but also in star clusters far out in the galactic halo (Matsumoto et al. 2001; Roberts et al. 2004; Farrell et al. 2009; Jonker et al. 2010). A large population of IMBHs might reside inside a galaxy halo, perhaps the leftover population of initial “seed” holes that never grew into the supermassive variety (SMBHs¹) hosted today in the nuclei of massive galaxies. The mechanism of seed formation is unknown. Seed holes may be produced by the direct collapse of $10^4 - 10^6 M_{\odot}$ primordial gas clouds, by the

collapse of the first nuclear star clusters, or be the remnants of $10^2 M_{\odot}$ Population III stars (e.g. Loeb & Rasio 1994; Madau & Rees 2001; Devecchi & Volonteri 2009). If we could directly observe the abundance, spatial distribution, and masses of IMBHs inside extragalactic halos, we would be able to constrain the process of SMBH seed formation that has hitherto been veiled in mystery.

We propose here to directly detect IMBHs by observing multiply imaged QSO-galaxy or galaxy-galaxy lens systems in the submillimeter band with high angular resolution ($\lesssim 0.3$ mas). Provided that the lensed source is sufficiently extended and the IMBHs inside the lensing galaxy are massive enough, then their gravitational force would significantly distort the lensed images (Inoue & Chiba 2003, 2006). Moreover, any star cluster or dark matter subhalo that surrounds an IMBH would also distort the lensed images at angular scales larger than the Einstein radius of the IMBHs. Using local distortions in the surface brightness of the lensed images, one can directly measure the position, mass scale, and gravitational potential surrounding the IMBHs.

* E-mail: kinoue@phys.kindai.ac.jp

† E-mail: valery@ucolick.org

‡ E-mail: silk@astro.ox.ac.uk

§ E-mail: pmadau@ucolick.org

¹ Here a “SMBH” means a black hole (BH) residing at the center of a main parent halo. If the host halo harbouring the BH belongs to a more massive parent halo, we call it an “IMBH”.

In this paper, we estimate the feasibility of mapping IMBHs in forthcoming observations. In Section 2, we describe a particle tagging technique to dynamically populate the N-body *Via Lactea II* (VLII) extreme-resolution simulation with IMBHs, and derive semi-analytic formulae for describing the surface mass and number density of IMBHs in the host halo. In Section 3, we estimate the strong lensing probability due to IMBHs in a lensing galaxy. We then describe the extended source effects and observational feasibility of direct detection in the QSO-galaxy lensing system RXJ1131-1231. We summarise our results in Section 4. In what follows, we assume a concordant cosmology with a matter density $\Omega_m = 0.272$, a baryon density $\Omega_b = 0.046$, a cosmological constant $\Omega_\Lambda = 0.728$, and a Hubble constant $H_0 = 70$, km/s/Mpc, which are obtained from the observed CMB, the baryon acoustic oscillations, and measurement of H_0 .

2 A POPULATION OF IMBHs

2.1 Simulation and tagging technique

VLII, one of the highest-resolution N-body simulations of the assembly of a Milky Way-sized galaxy halo to date (Diemand et al. 2008), provides an ideal set-up for the study of formation of IMBHs. VLII follows the hierarchical assembly of a dark halo of mass $M_{200} = 2 \times 10^{12} M_\odot$ at redshift $z = 0$ within $r_{200} = 402$ kpc (the radius which encloses an average mass density 200 times the mean cosmological matter density), with just over a billion particles and a force resolution of 40 pc. The simulation was performed with the parallel tree-code PKDGRAV2 (Stadel 2001). PKDGRAV2 uses a fast multipole expansion technique in order to calculate the forces with hexadecapole precision, and an adaptive leapfrog integrator. Expected to harbor a thin disk galaxy, VLII was selected to have no major mergers after $z = 1$. At the present epoch, VLII has a cuspy density profile and exhibits rich galactic substructure - the main host’s halo contains over 20,000 surviving subhalos with masses greater than $10^6 M_\odot$.

Central black holes are added to subhalos following the particle tagging technique detailed in Rashkov & Madau (2013) and quickly summarized here. In each of 27 snapshots of the simulation, chosen to span the assembly history of the host between redshift $z = 27.54$ and the present, all subhalos are identified and linked from snapshot to snapshot to their most massive progenitor: the subhalo tracks built in this way contain all the time-dependent structural information necessary for our study. We then identify the simulation snapshot in which each subhalo reaches its maximum mass M_{halo} before being accreted by the main host and tidally stripped. In each subhalo, the 1% most tightly bound dark matter particles are then “tagged” as stars at infall, following a set of simple prescriptions calibrated to reproduce the observed luminosity function of Milky Way satellites and the concentration of their stellar populations (Rashkov et al. 2012). We then measure the stellar line-of-sight velocity dispersion, σ_* , in each subhalo, and tag the most tightly bound central particle as a black hole of mass M_{BH} according to an extrapolation of the $M_{\text{BH}} - \sigma_*$ relation

of Tremaine et al. (2002),

$$M_{\text{BH}} = 8.1 \times 10^6 M_\odot \left(\frac{\sigma_*}{100 \text{ km s}^{-1}} \right)^4. \quad (1)$$

For stellar systems with $\sigma_* \leq 6 \text{ km s}^{-1}$, a minimum seed hole mass of $100 M_\odot$ is assumed. Any evolution of the tagged holes after infall is purely kinematical in character, as their satellite hosts are accreted and disrupted in an evolving Milky Way-sized halo. Black holes do not increase in mass after tagging, and are tracked down to the $z = 0$ snapshot. We assume that IMBHs only form in subhalos with a mass at infall $> M_{\text{min}}^s = 10^7 M_\odot$.

The merging process that produces each subhalo prior to its infall into the main host halo is important, as black hole binaries may form in the process. The asymmetric emission of gravitational waves produced during the coalescence of a binary black hole system is known to impart a velocity kick to the system that can displace the hole from the center of its host. The magnitude of the recoil will depend on the binary mass ratio and the direction and magnitude of their spins, and follows the prescriptions detailed in Guedes et al. (2011). When the kick velocity is larger than the escape speed of the host halo, a hole may be ejected into intergalactic space before becoming a Galactic IMBH. IMBHs that would have formed in halos whose merger history points to a kick event are therefore excluded from the final catalog (see Rashkov & Madau 2013 for details).

Since some of the subhalos will fall on trajectories that bring them closer to the center of the main VLII host, they might be completely disrupted after infall, leaving freely-roaming (“naked”) holes. Depending on the minimum halo mass that allows the formation of an IMBH, the numbers of formed, kicked, and stripped IMBHs will be different. Figure 1 shows an image of the projected distribution of IMBHs in today’s Galactic halo according to the above prescriptions. We find 1,070 naked IMBHs and 1,670 holes residing in dark matter satellites that survived tidal stripping. There are 50 IMBHs more massive than $10^3 M_\odot$, and about 2,500 holes at the minimum mass of $100 M_\odot$ (of which 950 are naked). Naked holes are more concentrated towards the inner halo regions as a consequence of the tidal disruption of infalling satellites. Indeed, within 10 kpc, most MBHs are naked.

2.2 Semi-analytic modeling

To generalize the numerical results of the previous section, we shall assume in the following that the distribution of IMBHs inside a lensing galaxy halo is spherically symmetric, and that the surface mass density σ_m and the surface number density σ_n are described by the following “universal profiles”,

$$\sigma_m(r) = \frac{\sigma_m(0)}{((r/r_c)^2 + 1) \exp[r/r_*]}, \quad (2)$$

$$\sigma_n(r) = \frac{\sigma_n(0)}{(r/r_c + 1) \exp[r/r_*]}, \quad (3)$$

where r_c represents a core radius and r_* denotes a cut-off radius at which the density starts to decay exponentially with increasing r . The “universal profiles” are much steeper than those of a singular isothermal sphere (SIS). Subhalos hosting IMBHs can be massive enough to experience dynamical friction, spiral in toward the center of the main host, be totally

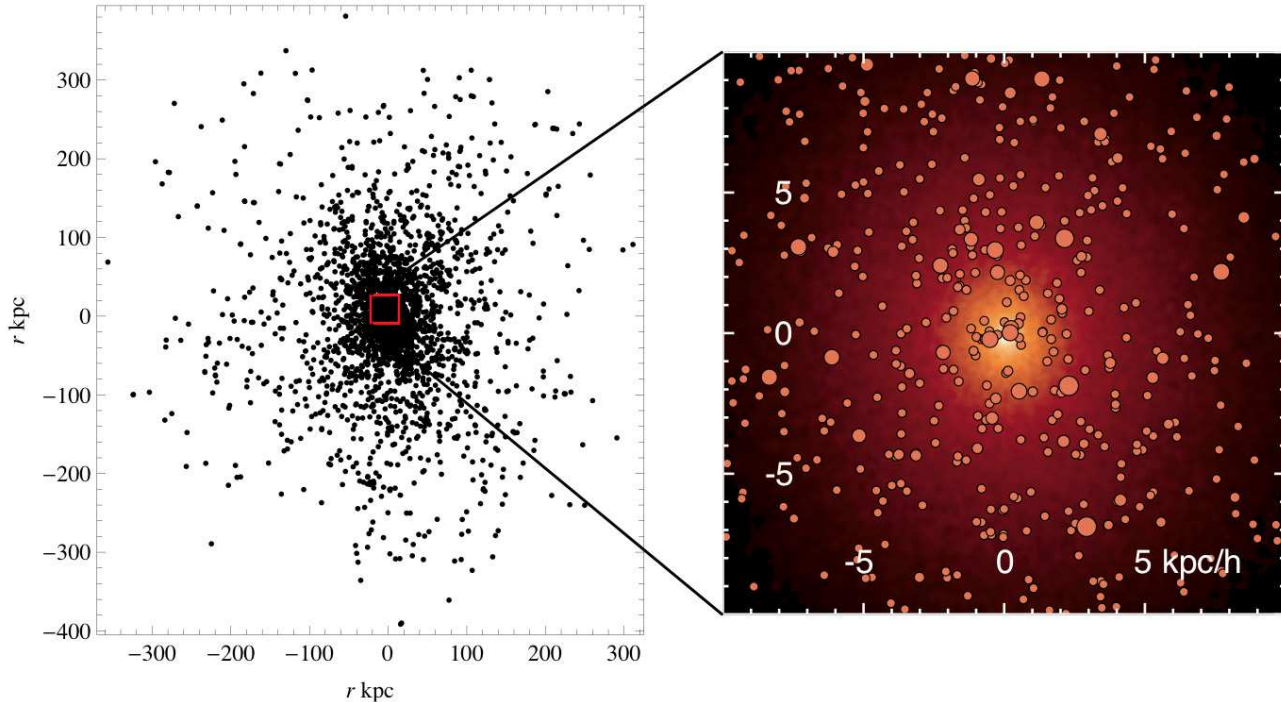


Figure 1. Plot of the distribution of IMBHs in the simulated Milky Way-sized halo. Each dot represents the position of an IMBH (left). The threshold of the minimum subhalo mass required for the formation of a seed hole is assumed to be $M_{\min}^s = 10^7 M_{\odot}$. The projected density of dark matter in the VLII simulation is plotted in a zoom-up image, where the size of each disk is proportional to the \log_{10} of the BH mass (right).

stripped of their dark matter, and deposit a naked IMBH into the center of the main host. As shown in Figure 2, most of IMBHs at $r \lesssim 10$ kpc are naked. We find that the surface mass density at $r \lesssim 10$ kpc is not significantly affected by M_{\min}^s .

The constants $\sigma_m(0)$ and $\sigma_n(0)$ can be estimated as follows. First, each halo is approximated as a spherically symmetric object with virial radius r_{200} . We assume that within r_{200} the halo density profile is given by that of an SIS with one dimensional velocity dispersion σ_v . Then we have

$$r_{200}(z) = \frac{\sigma_v}{H(z)\sqrt{50\Omega_m(z)}}, \quad (4)$$

where $\Omega_m(z)$ and $H(z)$ are the matter density parameter and the Hubble parameter at redshift z , respectively. The initial size of the halo is then

$$r_{ini} \approx 200^{1/3} r_{200}. \quad (5)$$

The correlation between the stellar velocity dispersion σ_v and mass M_{SMBH} of the supermassive black hole at the center is approximately given by

$$\left(\frac{M_{\text{SMBH}}}{10^8 M_{\odot}}\right) \sim \beta \times \left(\frac{\sigma_v}{200 \text{ km/s}}\right)^{\alpha}, \quad (6)$$

where $\beta = O(1)$ and $4 < \alpha < 5$. The mass of the SMBH at the nucleus of the Milky Way is $M_{\text{SMBH}} = 4 \times 10^6 M_{\odot}$. Then, the velocity dispersion of the spheroidal component is $\sigma_v = 88$ km/s and $r_{200} = 3.4 \times 10^2$ kpc at $z = 0$ provided that $\alpha = 4.24$ and $\beta = 1.32$ (Gültekin et al. 2009). We also assume that the total mass of IMBHs within r_{200} is given by

$M_{\text{IMBH}}(< r_{200}) = f M_{\text{SMBH}}$, where $f = 0.1 - 1$. Then from equations (2) and (6), we have

$$\sigma_m(0) \approx \frac{\beta f (\sigma_v/200 \text{ km/s})^{\alpha}}{2\pi r_c^2 (\ln(r_{200}/r_c) + 1/2)} \times 10^8 M_{\odot}. \quad (7)$$

If we adopt $f = 0.2$, the analytically estimated surface mass density σ_m fits the simulated values well (see Fig. 2). We find that the surface mass density in the neighborhood of the center does not change much even if one changes the threshold M_{\min}^s .

Second, we assume that the seed of an IMBH is formed at a redshift of $z = 20$ inside a host halo with a mass of $M > M_{\min}^s$, and each seed grows almost independently. Then the approximated virial radius of the halo is $\tilde{r}_{200}(z = 20) = 3.3 \times 10^2$ pc. Assuming an SIS profile, the maximal circular velocity of a host halo is estimated as $V_{\max} = \sqrt{2}\sigma_v = 10H\tilde{r}_{200} = 12$ km/s. At $z = 20$, the number density of subhalos with maximal velocity larger than V_{\max} is approximately given by

$$\begin{aligned} n(> V_{\max}) &= \frac{A}{V_{\max}^3}, \\ A(z = 20) &= 1.43 \times 10^5 \left(h^{-1} \text{Mpc}/(\text{km/s})\right)^{-3}, \end{aligned} \quad (8)$$

provided that $V_{\max} \ll 1000$ km/s (Klypin et al. 2011).

For the Milky Way-sized halo in VLII, the initial radius is estimated as $r_{ini}(z = 20) = 1.65$ Mpc/h. Assuming that all the halos with mass $> 10^7 M_{\odot}$ contain an IMBH seed, the total number of IMBH seeds inside a lensing galaxy halo

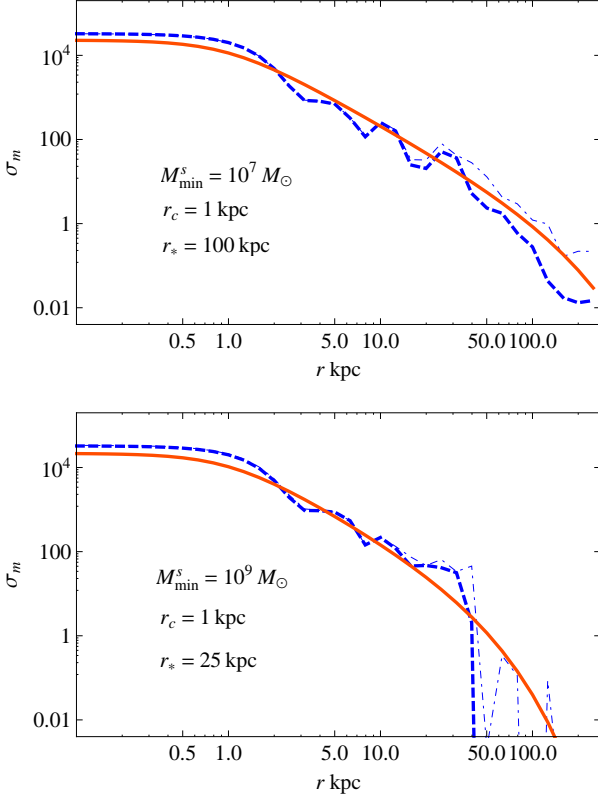


Figure 2. Surface mass density of IMBHs in the simulated Milky Way-sized halo. The dashed and dot-dashed curves correspond to the naked and the total (naked plus hosted-in-substructure) IMBHs in our numerical simulations, respectively. The solid curves represent fitted “universal profiles” in which the total mass of IMBHs coincides with that of our simulated results. This curve is also obtained if we assume $f = 0.2$. The distribution of simulated IMBHs is smoothed by a Gaussian window function $W(r) = \exp[-r^2/(2r_c^2)]$, where $r_c = 1$ kpc. The total masses of IMBHs (naked plus hosted-in-substructure) are $9 \times 10^5 M_\odot$ (top) and $8 \times 10^5 M_\odot$ (bottom).

is estimated as

$$\begin{aligned} N(> V_{max} = 12 \text{ km/s}) &= \frac{A(z=20)}{(V_{max} = 12 \text{ km/s})^3} \times \frac{4}{3} \pi r_{ini}^3 \\ &= 1.8 \times 10^3. \end{aligned} \quad (9)$$

Note that $N(> V_{max})$ is proportional to r_{200}^3 . If the total number of IMBHs within r_{200} does not change much, then the surface number density at the center is

$$\sigma_n(0) \approx \frac{N(> V_{max})}{2\pi r_{200} r_c}. \quad (10)$$

Thus $\sigma_n(0)$ is proportional to r_{200}^2 or σ_v^2 if r_c does not depend on r_{200} . As shown in Figure 3, the “universal profile” fits the simulation well if the total number of IMBHs coincides with that of the simulation. If $\sigma_n(0)$ in equation (10) is used, however, the surface number density is systematically reduced by a factor of 2 – 5 in comparison with the simulation. This difference may be due to the strong clustering of massive halos.

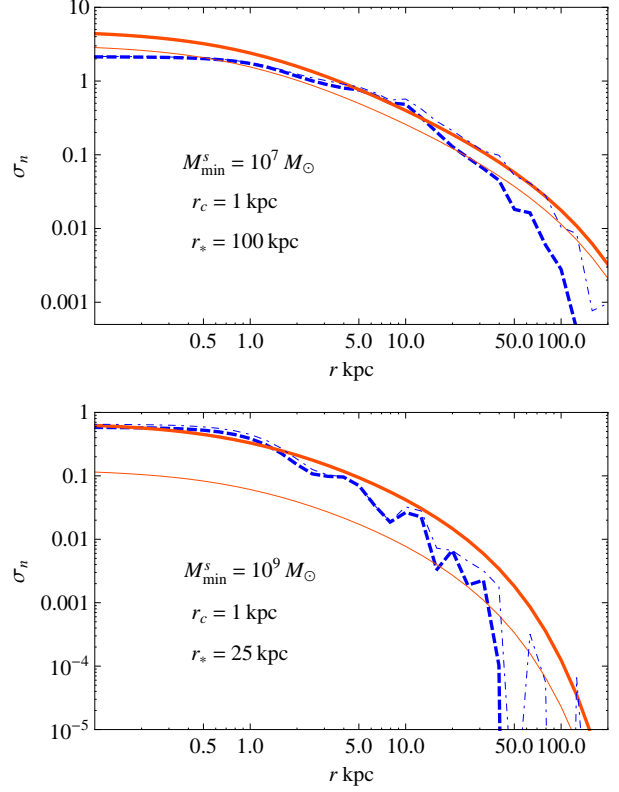


Figure 3. Surface number density of IMBHs in the simulated Milky Way-sized halo. The dashed and dot-dashed curves correspond to the naked and the total (naked plus hosted-in-substructure) IMBHs in our numerical simulations, respectively. The solid curves represent fitted “universal profiles” in which the total number of IMBHs coincides with that of our simulated results (bold solid) and that of our semi-analytically estimated values (thin solid). The distribution of simulated IMBHs is smoothed by a Gaussian window function $W(r) = \exp[-r^2/(2r_c^2)]$, where $r_c = 1$ kpc.

3 LENSING EFFECT

3.1 Lensing probability

The Einstein angular radius θ_E of a point mass with a mass M is written in terms of angular diameter distances: to the lens D_L , to the source D_S , and between the lens and the source D_{LS} as

$$\theta_E \sim 3 \times \left(\frac{M}{10^6 M_\odot} \right)^{\frac{1}{2}} \left(\frac{D_L D_S / D_{LS}}{\text{Gpc}} \right)^{-\frac{1}{2}} \text{ mas}. \quad (11)$$

Therefore, a radio interferometer with resolution of 3 mas can easily resolve the distortion of an image within the Einstein ring for a point mass $M \sim 10^6 M_\odot$.

The strong lensing cross section due to an IMBH is proportional to M . Therefore, the lensing probability p is given by the ratio between the surface mass density of IMBHs and that of a lensing galactic halo at $r = r_E = D_L \theta_E$. From equations (2) and (7), we have

$$p = \frac{\sigma_m(\text{IMBH})}{\sigma_m(\text{SIS})} \Big|_{r=r_E} \propto \frac{\sigma_v^\alpha}{\sigma_v^2 r_E} \propto f \sigma_v^{\alpha-4}, \quad (12)$$

where $\sigma_m(\text{IMBH})$ and $\sigma_m(\text{SIS})$ denote the surface mass den-

sity of IMBHs and that of an SIS, respectively. Similarly, the mean mass \bar{M} of an IMBH at $r = r_E$ satisfies

$$\bar{M} = \frac{\sigma_m(\text{IMBH})}{\sigma_n(\text{IMBH})} \Big|_{r=r_E} \propto f \sigma_v^{\alpha-4}. \quad (13)$$

Thus the lensing probability and the Einstein radius are larger for halos with larger velocity dispersion as long as $\alpha > 4$ and equations (2) and (3) hold. As the Einstein radius of an IMBH is proportional to $D_L^{-1/2}$, lens systems with small D_L are more suitable as targets.

3.2 Extended source effect

If a perturber is spatially extended, then the lensing effect is different from that of a point mass. The density profile of a perturber can be reconstructed from a local mapping between the observed image and the non-perturbed image obtained from the prediction of the macrolens. In fact, the power of the radial density profile of the perturbers can be reconstructed from the perturbed images within the Einstein ring of the perturber (Inoue & Chiba 2005a). In this way, one could make a distinction between an IMBH and a CDM subhalo. Furthermore, from distortion outside the Einstein ring of the perturber, the degeneracy between the perturber mass and the distance can be broken provided that the Einstein radius of the perturber is sufficiently smaller than that of the primary macrolens (Inoue & Chiba 2005b). The precise measurement of spatial variation in the surface brightness of lensed images provides us with plenty of information about the mass, abundance, and spatial distribution of IMBHs.

3.3 Simulation for RXJ1131-1231

To estimate the observational feasibility of direct detection of IMBHs, we adopt a QSO-galaxy lensing system RXJ1131-1231 as a target since this system has a massive lensing halo at relatively small redshift. The redshifts of the source and the lens are $z_S = 0.658$ and $z_L = 0.295$ (Sluse et al. 2003), respectively. To model the macro-lens, we adopt a singular isothermal ellipsoid (SIE) in a constant external shear field in which the isopotential curves in the projected surface perpendicular to the line-of-sight are ellipses (Kormann et al. 1994; Inoue & Takahashi 2012). The IMBHs inside the lensing halo are modeled as point masses. Using the observed mid-infrared fluxes, the position of the lensed images and the centroid of the lensing galaxy, the velocity dispersion for the best-fit model is estimated as $\sigma_v = 3.5 \times 10^2$ km/s. From the $M - \sigma$ relation with $\alpha = 4.24$ and $\beta = 1.32$ (Gültekin et al. 2009), the total mass of IMBHs within r_{200} is $M_{\text{IMBH}} = 1.5f \times 10^9 M_\odot$. Then the lensing probability is $p = 5f \times 10^{-4}$. The mean mass of the IMBH at $r = r_E = 5.6$ kpc/h is $\langle M_{\text{IMBH}} \rangle = 2f \times 10^5 M_\odot$ and the corresponding Einstein radius is $\theta_E = \sqrt{f}$ mas. Therefore, if the angular resolution is $< \sqrt{f}$ mas, we would be able to detect an imprint of IMBHs in the lensed Einstein ring of dust emission if the lensed image has an area $> 2000f^{-1}$ mas².

To estimate observational feasibility, we use the simulated data of IMBHs for a Milky Way-sized halo with $M_{\text{min}}^s = 10^7 M_\odot$ and scale up the mass of each IMBH by a ratio between the total mass of the SMBH for RXJ1131-1231 ($= 1.5 \times 10^9 M_\odot$) and that for the Milky Way-sized

halo ($= 4 \times 10^6 M_\odot$). In this model, we find that the ratio between the mass fraction of all IMBHs to that of a SMBH in the center is $f = 0.2$. The most massive IMBH has a mass of $M_{\text{IMBH}} = 7 \times 10^7 M_\odot$. Taking into account the logarithmic correction to σ_v in equation (7), the distance of each particle from the center is scaled up by a factor

$$\begin{aligned} \gamma &\approx \left(\frac{\ln(\sigma_v(\text{RXJ1131})/(\sqrt{50}H(z=0.295)r_c))}{\ln(\sigma_v(\text{MW})/(\sqrt{50}H(z=0)r_c))} \right)^{1/2} \\ &= 1.05, \end{aligned} \quad (14)$$

where we assume that $r_c = 1$ kpc. As shown in Figure 4, we find that massive “naked” IMBHs with masses in the range of $O(10^{5-6}) M_\odot$ are observable if the radius of the dust emitting region around the QSO is ~ 500 Mpc and the angular resolution is < 1 mas. The area of the lensed arc is found to be $\sim 6 \times 10^5$ mas². Thus we expect $> O(10)$ “naked” IMBHs inside the lensed arc if $f > 0.2$.

Even if IMBHs reside in places far from the brightest part of the Einstein ring of dust emission, the surface brightness of the lensed image that is sufficiently close to the position of an IMBH is the same as that of the brightest region in the Einstein ring. It is easily distinguished from other sources as the spatial gradient of the surface brightness is extremely large near the position of an IMBH.

4 SUMMARY

Based on numerical simulations of IMBH formation in a Milky-way sized halo, we have found that the surface mass density and number density of IMBHs have power-law dependences on the distance from the center of the host halo if smoothed on scales of ~ 1 kpc. Most of the black holes orbiting close to the center are freely roaming as they have lost their surrounding dark mass during infall due to tidal stripping. Assuming the surface mass density and number density have such power-law dependences, the strong lensing probability due to free roaming IMBHs in a massive lensing galaxy such as RXJ1131-1231 is $\sim O(10^{-4})$. The next generation submillimeter telescopes with high angular resolution ($\lesssim 0.3$ mas) will be capable of directly mapping these freely roaming IMBHs with a mass of $\sim 10^6 M_\odot$.

In addition to IMBHs in the lensing galaxy, SMBHs with a mass of $\gtrsim 10^6 M_\odot$ inside halos in the line-of-sight may also be observable, especially in systems that show anomalies in the flux ratios (Inoue & Takahashi 2012). In this case, some distortion in the lensed image due to the host halo is expected.

By measuring the local distortion of lensed extended images with high angular resolution, we will be able to determine the mass, abundance, and density profile of the IMBHs present in the lensing galaxy. Direct detection of IMBHs will shed new light on the formation process of SMBH seeds which has hitherto been shrouded from view.

5 ACKNOWLEDGMENTS

This work was supported by the NSF through grant OIA-1124453, and by NASA through grant NNX12AF87G. This research was also supported in part by ERC project 267117

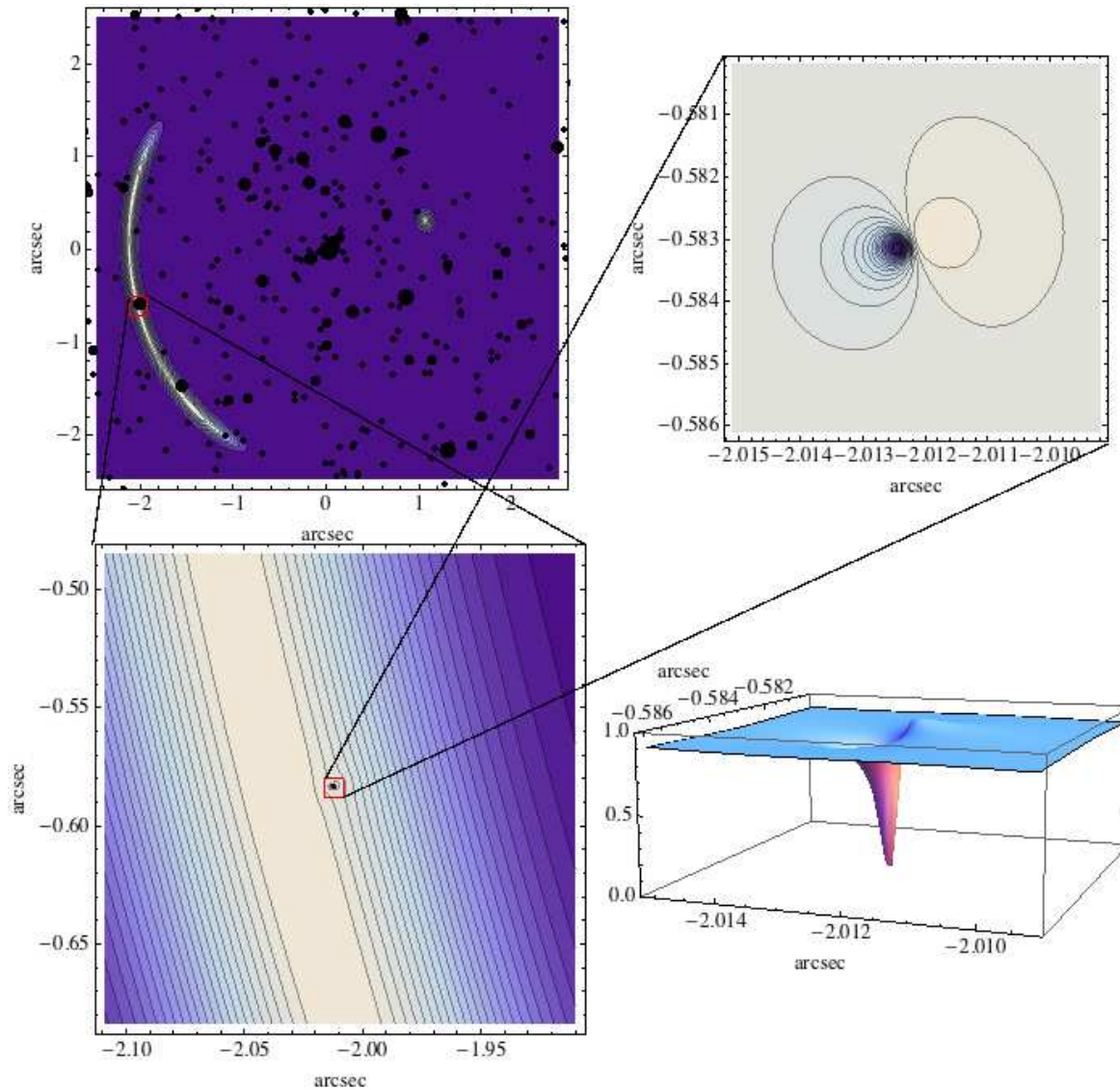


Figure 4. Simulated lensed images of RXJ1131-1231. The black dots in the top left panel show the positions of IMBHs in the lensing galaxy and the dot size is proportional to $\log_{10}(M_{\text{IMBH}})$. The other panels show the contour and 3D maps of the surface brightness centered at the angular position of an IMBH with a mass of $1.4 \times 10^6 M_{\odot}$ that produces a “black hole”. We assume that the dust emitting region has a circular gaussian luminosity profile with a 1σ radius $r = 500$ pc. The numbers of contours representing the surface brightness are 10 (top left), 25 (bottom left), 25 (top right).

(DARK) hosted by Université Pierre et Marie Curie - Paris 6.

REFERENCES

- Devecchi B., Volonteri M., 2009, *The Astrophysical Journal*, 694, 302
- Diemand J., Kuhlen M., Madau P., Zemp M., Moore B., Potter D., Stadel J., 2008, *Nature*, 454, 735
- Farrell S. A., Webb N. A., Barret D., Godet O., Rodrigues J. M., 2009, *Nature*, 460, 73
- Guedes J., Madau P., Mayer L., Callegari S., 2011, *The Astrophysical Journal*, 729, 125
- Gültekin K., Richstone D. O., Gebhardt K., Lauer T. R., Tremaine S., Aller M. C., Bender R., Dressler A., Faber S. M., Filippenko A. V., Green R., Ho L. C., Kormendy J., Magorrian J., Pinkney J., Siopis C., 2009, *The Astrophysical Journal*, 698, 198
- Inoue K. T., Chiba M., 2003, *The Astrophysical Journal Letter*, 591, L83
- Inoue K. T., Chiba M., 2005a, *The Astrophysical Journal*, 634, 77
- Inoue K. T., Chiba M., 2005b, *The Astrophysical Journal*, 633, 23
- Inoue K. T., Chiba M., 2006, *Annual reports by Research Institute for Science and Technology*, 18, 11
- Inoue K. T., Takahashi R., 2012, *Monthly Notices of Royal Astronomical Society*, 426, 2978
- Jonker P. G., Torres M. A. P., Fabian A. C., Heida M., Miniutti G., Pooley D., 2010, *Monthly Notices of Royal*

- Astronomical Society, 407, 645
- Klypin A. A., Trujillo-Gomez S., Primack J., 2011, *The Astrophysical Journal*, 740, 102
- Kormann R., Schneider P., Bartelmann M., 1994, *Astronomy and Astrophysics*, 284, 285
- Loeb A., Rasio F. A., 1994, *The Astrophysical Journal*, 432, 52
- Madau P., Rees M. J., 2001, *The Astrophysical Journal Letter*, 551, L27
- Matsumoto H., Tsuru T. G., Koyama K., Awaki H., Canizares C. R., Kawai N., Matsushita S., Kawabe R., 2001, *The Astrophysical Journal Letter*, 547, L25
- Rashkov V., Madau P., 2013, in preparation
- Rashkov V., Madau P., Kuhlen M., Diemand J., 2012, *The Astrophysical Journal*, 745, 142
- Roberts T. P., Warwick R. S., Ward M. J., Goad M. R., 2004, *Monthly Notices of Royal Astronomical Society*, 349, 1193
- Sluse D., Surdej J., Claeskens J. F., Hutsemekers D., Jean C., Courbin F., Nakos T., Billeres M., Khmil S. V., 2003, *Astronomy and Astrophysics*, 406, L43
- Stadel J. G., 2001, Ph.D. Thesis, University of Washington
- Tremaine S., Gebhardt K., Bender R., Bower G., Dressler A., Faber S. M., Filippenko A. V., Green R., Grillmair C., Ho L. C., Kormendy J., Lauer T. R., Magorrian J., Pinkney J., Richstone D., 2002, *The Astrophysical Journal*, 574, 740